IN-VENTO 2014
XIII Conference of the Italian Association for Wind Engineering
22-25 June 2014, Genova, Italy

Efficient estimation of the high-order response statistics of a wind-excited oscillator with nonlinear velocity feedback

Vincent Denoël[1], Luigi Carassale[2]

[1]Structural Engineering Division, University of Liège, Belgium
[2]Dept. of Civil Chemical and Environmental Engineering, University of Genova, Italy
Corresponding author: Vincent Denoël, Vincent Denoël, v.denoel@ulg.ac.be

Abstract

The point-like quasi-steady aerodynamic loading in a turbulent flow is formally expressed as a function of the squared relative velocity between the fluid and the investigated structure. The three major terms governing the low-order statistics of the response are known to be related to the average loading, the linear turbulent loading and the aerodynamic damping. The three other terms in the loading, namely the quadratic turbulence term, the parametric velocity feedback term and the squared velocity term, may significantly affect the higher order statistical cumulants of the response. These latter two sources of fluid-structure interaction are usually disregarded, by lack of efficient simulation tools, except a Monte Carlo simulation of the nonlinear equation. In this paper, we provide a formal analysis of the complete nonlinear model, including thus all six terms, but mainly focusing on the importance of the two nonlinear coupling terms of the loading. Closed form solutions of the response are derived for a second-order Volterra model of this problem, under the assumption of different timescales in the loading and in the structural behaviour. Two major outcomes of the analysis are, on the one hand, that the squared structural velocity term has no influence on the cumulants of the response up to order 4 and, on the other hand, that the parametric velocity feedback acts as a reduction of the non Gaussianity of the response.

1 Introduction

The response of civil engineering structures to the wind turbulence is a multiple timescale process. Indeed, in a linear context, the structural response to very low frequency turbulence excitation may be approached by a sum of two components, a background component associated with the slow dynamics of the excitation and a fast resonant component associated with the structural timescale (Davenport, 1961).

The stochastic structural analysis of a linear structure subject to a stationary excitation, such as the wind turbulence, is usually performed with a spectral approach. While offering a clear understanding of the structural behaviour and the dispatching of energy in the different timescales, this approach also sidesteps the heavy generation of the wind velocity or pressure time histories. The stochastic approach is a useful tool to determine the Gaussian, but also non-Gaussian, response of a linear system. One drawback perhaps is that the evaluation of high-order statistics requires a multi-dimensional integration of spectral densities in spaces whose dimension increases with the order of the cumulants of the response under investigation. The application of the method in the context of non-Gaussian responses thus turns out to be challenging, from a computational viewpoint. This drawback is partly circumvented by considering the existence of the different timescales in the response. Doing so, the multiplicity of the integrals to be computed is decreased by one, which substantially speeds up the computation (Denoël, 2014).

In this paper, the concept described above is extended to the study of a linear oscillator whose excitation is defined as a quadratic function of the wind-structure relative velocity. The analysis still relies on a spectral approach and the structural system is modelled as a Volterra system (e.g. Schetzen, 1980). Developments are limited to the second-order Volterra operator which is shown to be accurate enough for the statistics up to order 4. The efficiency of the method is discussed with the determination of the first four cumulants of the response. The quality of the result is assessed in terms of accuracy with respect to a reference solution obtained through Monte Carlo simulation. Under the quasi-steady assumption, the response of a point-like single degree-of-freedom structure subject to a 1-dimensional wind turbulence is governed by the nonlinear second order differential equation

$$m\ddot{x} + c\dot{x} + kx = \frac{1}{2}\rho C_d A\left(U + u - \dot{x}\right)^2 \tag{1}$$

where $x(t)$ is the structural displacement, m, c and k are mass, viscosity and stiffness, respectively, U is the mean wind velocity and $u(t)$ a Gaussian zero-mean random process representing the wind velocity fluctuation; ρ, A and C_d are, respectively, the air density, the area of the structure exposed to the wind and the aerodynamic drag coefficient. The overhead dot denotes differentiation with respect to time t. The nonlinearity of this equation results from the squared structural velocity $\dot{x}^2(t)$ and the parametric excitation $-2\dot{x}(t)u(t)$ terms obtained in the right-hand side after expansion.

The zero-mean Gaussian turbulence process $u(t)$ is fully described by its power spectral density $S_u(\omega)$. Following Kolmogorov's energy cascade, typical models for the turbulence decrease as $\omega^{-5/3}$ in the high-frequency range. This non Markovian behaviour makes any stochastic method based on the FPK equation and moment equation rather intricate since a proper approximation with a Markovian process has to be formulated. This argument drove the solution procedure of the considered problem toward spectral methods. It is thus possible to handle realistic power spectral densities of the wind turbulence such as

$$S_u\left(\omega;\frac{L}{U}\right) = \sigma_u^2 \frac{0.546\dfrac{L}{U}}{\left(1+1.64\dfrac{L}{U}|\omega|\right)^{5/3}} \tag{2}$$

in which L represents the integral length scale and σ_u the standard deviation of the turbulence velocity.

This problem might be formulated in a dimensionless manner leading to the governing equation

$$\tilde{x}'' + 2\left(\xi_s + \xi_a\right)\tilde{x}' + \tilde{x} = \frac{1}{2I_u} + \tilde{u} + \frac{1}{2}I_u\tilde{u}^2 - 2I_u\xi_a\tilde{u}\tilde{x}' + 2I_u\xi_a^2\tilde{x}'^2 \tag{3}$$

where the following dimensionless quantities are used

$$\begin{aligned} &\tilde{x} = \frac{k}{\rho A C_d I_u U^2}x, && \tilde{u} = \frac{u}{\sigma_u}, && \tilde{t} = \sqrt{\frac{k}{m}}t = \omega_0 t, \\ &\xi_s = \frac{c}{2m\omega_0}, && \xi_a = \frac{\rho A C_d U}{2m\omega_0}, && \alpha = \frac{U}{L\omega_o} \end{aligned} \tag{4}$$

and where a prime $'$ denotes differentiation with respect to the nondimensional time $\tilde{t}$. The power spectral density $S_{\tilde{u}}(\tilde{\omega};\alpha)$ of the dimensionless turbulence velocity $\tilde{u}$ is a function of the dimensionless frequency $\tilde{\omega}$ and of the small parameter α, which is the ratio of the characteristic turbulence frequency U/L and the structural natural frequency ω_0. The two coefficients ξ_s and ξ_a represent the structural and aerodynamic damping coefficients.

This formulation indicates that the solution of the problem at hand may evolve in different regimes, depending on the relative smallness of ξ_s, ξ_a and α. These three numbers are typically in the range [10^{-3}; 10^{-1}]. A fourth small parameter of the problem is the turbulence intensity I_u, usually in the range [10%; 30%], which scales the quadratic turbulence term and the nonlinear feedback terms on the right hand side of Eq. (3). The dimensionless version of the governing equation readily shows that the quadratic velocity term x'^2 is one order of magnitude smaller than its left neighbour ux', the parametric excitation term, which presumably indicates that the former one would yield negligible contribution to the response. This is to be proved with a more formal derivation. Although the dimensionless version of the governing equation is definitely more convenient to identify the leading physics and its limiting cases, the paper is mainly developed with physical quantities, so as to provide a simpler understanding.

2 Second order Volterra model

2.1 The Volterra Frequency Response Functions

Inspired by former works (Carassale & Kareem, 2010), it is chosen to model the response of this nonlinear problem with a second order Volterra model. This choice is validated in Section 5, with the typical orders of magnitude of the parameters encountered in wind engineering applications.

In this framework, the response $x(t)$ is approximated as

$$x(t) \simeq x_o + x_1(t) + x_2(t) \tag{5}$$

where $x_1(t)$, respectively $x_2(t)$, is defined as the first (resp. second) order convolution of the zero-mean Gaussian input $u(t)$ with the Volterra kernel $h_1(t)$, respectively $h_2(t)$. In a stationary setting, this definition is advantageously translated into the frequency domain with the symmetrical Volterra frequency response functions (VFRF) $H_1(\omega)$ and $H_2(\omega_1,\omega_2)$.

These functions need to be established for the specific nonlinearity of the problem under consideration. This may be achieved with the harmonic probing technique (Bedrosian & Rice, 1971) or with the systematic procedure presented in Carassale & Kareem (2010). The same procedure as that developed in the later one has been used to derive the VFRFs as:

$$\begin{aligned} H_1(\omega) &= \frac{\rho C_d AU}{D(\omega) + j\omega\rho C_d AU}, \\ H_2(\omega_1,\omega_2) &= \frac{\rho C_d A}{2} \frac{\left(1 - j\omega_1 H_1(\omega_1)\right)\left(1 - j\omega_2 H_1(\omega_2)\right)}{D(\omega_1+\omega_2) + j(\omega_1+\omega_2)\rho C_d AU} \end{aligned} \tag{6}$$

where $D(\omega) = -m\omega^2 + j\omega c + k$ is the inverse of the FRF defining the mechanical part of the system.

These frequency response functions are sketched in Figure 1. The first one corresponds to the classical frequency response function of a linear oscillator, with additional aerodynamic damping. The second represents the interaction between the different harmonics in the response, especially the filtering of pairs of harmonics (ω_1, ω_2) that fall out of the band $|\omega_1 + \omega_2| \simeq \omega_o$.

2.2 Cumulants of the stationary response

In a second-order Volterra model, the total response is expressed as the sum in Eq. (5) involving the 0^{th}-order constant term x_0, together with the fluctuating terms $x_1(t)$ and $x_2(t)$. When the input $u(t)$ is a stationary random process, the statistical properties of the total response $x(t)$ may be expressed in terms of its cumulants, which in turn can be written as functions of the cumulants of $x_1(t)$ and $x_2(t)$. Using some classical developments in the theory of probability (e.g. Papoulis, 1965) under the hypothesis that $u(t)$ is Gaussian distributed, we obtain

$$\begin{aligned} \kappa_2[x] &= \kappa_2[x_1] + \kappa_2[x_2] \\ \kappa_3[x] &= 3\kappa_3[x_1, x_1, x_2] + \kappa_3[x_2] \\ \kappa_4[x] &= 6\kappa_4[x_1, x_1, x_2, x_2] + \kappa_4[x_2] \end{aligned} \tag{7}$$

where $\kappa_k[\bullet]$ (when used with a single argument) represents the k^{th}-order cumulant of its argument and $\kappa_k[\bullet,...,\bullet]$ represents the k^{th}-order cross-cumulant associated with the product of the arguments.

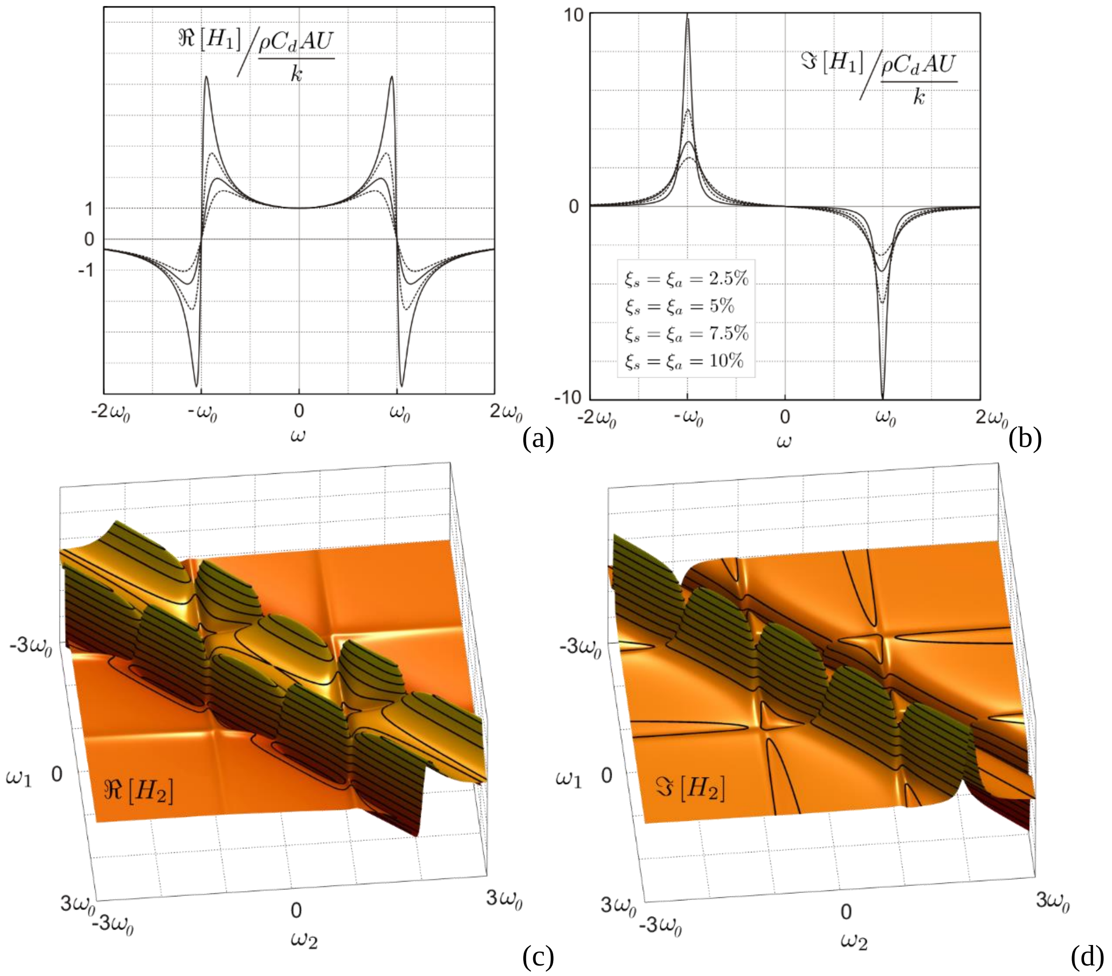

Figure 2. Second-order frequency response function ($\xi_s = \xi_a = 5\%$).

An analysis of the orders of magnitude of the two terms that compose each cumulant of the response reveals that the second terms in the expressions given in (7) are negligible in front of the first terms, at least for the small realistic values of the aerodynamic damping ξ_a encountered in typical wind engineering applications. The formal demonstration of this statement goes beyond the scope of this paper, but is available in Denoël and Carassale (2014) together with a deeper investigation of this problem.

Intuitively however, the second order response $x_2(t)$ is one or several orders of magnitude smaller than the first order response $x_1(t)$. The ratio of these two actually scales with the aerodynamic damping ξ_a. As a consequence, in Eq. (7), the cross-cumulant, involving more factors in $x_1(t)$ than the unilateral cumulants of $x_2(t)$ are expected to be leading.

2.3 Power spectral density and higher order spectra of the response

The power spectral density of the total response $x(t)$ of a second-order Volterra model reads

$$S_x(\omega) = \left|H_1(\omega)\right|^2 S_u(\omega) + 2\int_{-\infty}^{+\infty} \left|H_2(\omega_1, \omega-\omega_1)\right|^2 S_u(\omega_1) S_u(\omega-\omega_1)\,\mathrm{d}\omega_1 \tag{8}$$

where $S_u(\omega)$ is the power spectral density of the turbulence, while H_1 and H_2 represent the Volterra frequency response functions, as given in (6).

The integration of the power spectral density $S_x(\omega)$ provides the second cumulant of the total response

$$\kappa_2[x] = \int_{-\infty}^{+\infty} S_x(\omega)\mathrm{d}\omega \tag{9}$$

Substitution of (8) into (9) indicates that the cumulant of the response is composed of two terms, as hinted by (7) anyway. The first one, involving $|H_1(\omega)|$, is responsible for the linear counterpart of the response $\kappa_2[x_1]$, while the second term, involving the second-order frequency response function $|H_2(\omega_1,\omega_2)|$ provides the second contribution $\kappa_2[x_2]$ to the total cumulant, after integration along the real axis. Following the former observation that the second terms in (7) are negligible, the second term in the power spectral density of the total response is dropped.

It finally turns out that the second order response is that of a linear system whose total damping is represented by the sum of the structural and aerodynamic damping. In this context, there exists a classical way to bypass the numerical integration of $S_x(\omega)$ in (9). It is based on the background/resonant decomposition of the response, a two-timescale approximation of the response usually attributed to the pioneering works of Davenport (1961). In this method, the variance of the response is simply expressed as the sum of a background and a resonant component as

$$\kappa_2[x] \simeq \kappa_2[x_1] \simeq (1+r)\kappa_{2,B} \tag{10}$$

where

$$\kappa_{2,B} = \left(\frac{\rho C_d A U \sigma_u}{k}\right)^2; \quad r = \frac{S_u(\omega_o)}{\sigma_u^2}\frac{\pi\omega_o}{2(\xi_s+\xi_a)} \tag{11}$$

are readily interpreted as the background response and the resonant-to-background ratio.

One major advantage of this two-timescale method is that it sidesteps any integration and offers an approximate solution of the problem at no computational costs. Extension of this method to higher-order statistics was the key motivation for the consideration of this problem as a Volterra model.

Similarly to the power spectral density, the bispectrum of the total response $x(t)$ is composed of two terms, among which only the first one is retained in the analysis, as it is responsible for the contribution $3\kappa_3[x_1, x_1, x_2]$ to the third cumulant. The bispectrum of the response is thus approximated as

$$\begin{aligned} B_x(\omega_1,\omega_2) \;=\; & 2H_1(-\omega_1-\omega_2)H_1(\omega_1)H_2(\omega_1+\omega_2,-\omega_1)S_u(\omega_1+\omega_2)S_u(\omega_1)+ \\ & +2H_1(-\omega_1-\omega_2)H_1(\omega_2)H_2(\omega_1+\omega_2,-\omega_2)S_u(\omega_1+\omega_2)S_u(\omega_2)+ \\ & +2H_1(\omega_1)H_1(\omega_1)H_2(-\omega_1,-\omega_2)S_u(\omega_1)S_u(\omega_2) \end{aligned} \tag{12}$$

and the third cumulant of the response is approximated by

$$\kappa_3[x] \simeq 3\kappa_3[x_1,x_1,x_2] = \int_{-\infty}^{+\infty}\int_{-\infty}^{+\infty} B_x(\omega_1,\omega_2)\mathrm{d}\omega_1\omega_2 \tag{13}$$

Similarly again, the trispectrum of the total response $x(t)$ is composed of two terms, among which only the first one is considered. In this simplified version, it reads

$$\begin{aligned} T_x(\omega_1,\omega_2,\omega_3)=4\sum_{\substack{\alpha,\beta,\gamma=1,2,3\\ \alpha\neq\beta\neq\gamma}} & H_1(\omega_\alpha)S_u(\omega_\alpha)\Big[H_1(\omega_\beta)H_2(-\omega_\alpha,-\omega_\beta-\omega_\gamma)H_2(\omega_\beta+\omega_{\alpha_3},-\omega_\beta)S_u(\omega_\beta)S_u(\omega_\beta+\omega_\gamma)+ \\ & +H_1(-\omega_\alpha-\omega_\beta-\omega_\gamma)H_2(-\omega_\alpha,\omega_\alpha+\omega_\gamma)H_2(\omega_\alpha+\omega_\beta+\omega_\gamma,-\omega_\alpha-\omega_\gamma)S_u(\omega_\alpha+\omega_\beta+\omega_\gamma)S_u(\omega_\alpha+\omega_\gamma)\Big] \end{aligned} \tag{14}$$

where the summation is performed on all six possible permutations of the indexes α, β, γ = 1, 2, 3. The fourth cumulant of the response is thus approximated by

$$\kappa_4[x] \simeq 6\kappa_4[x_1, x_1, x_2, x_2] = \int_{-\infty}^{+\infty}\int_{-\infty}^{+\infty}\int_{-\infty}^{+\infty} T_x(\omega_1, \omega_2, \omega_3) \mathrm{d}\omega_1 \mathrm{d}\omega_2 \mathrm{d}\omega_3 \tag{15}$$

The purpose of the rest of the paper is to provide simple expressions for the integrals in (13) and (15).

3 Multiple Scale Spectral Analysis & Analysis of the Model

3.1 Cumulants of the response

The multiple timescale spectral analysis is a recent technique that allows decreasing by one (at least) the order of integration in the determination of the cumulants of the response. It hinges on the timescales separation between the loading and the structure and is able to deal with linear/nonlinear structures, stationary/evolutionary problems, SDOF/MDOF problems, and is fundamentally not limited regarding the statistical order (Denoël, 2014). The method is elaborated in the frequency domain and is not contingent upon the markovianity of the loading process; it thus deals with any complex analytical expression of the power spectral density of the loading –such as those that characterize the wind turbulence– without any artefact. The technique actually generalizes the background/resonant decomposition of the variance (Davenport, 1961) and the background/biresonant decomposition of the third cumulant (Denoël, 2011) of the response of a single degree-of-freedom linear system subject to slow stochastic loading.

Application of the general method requires the identification, in the response spectra, of the different components to the response. Among them the background component is easily identified. Its trivial subtraction from the initial response spectra leaves us with resonant and mixed background/resonant terms. Examples of applications in (Denoël, 2014) give some hints on how to determine and approximate these components.

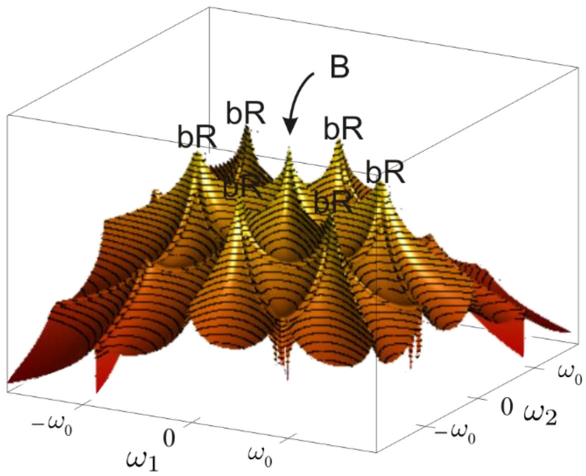

Figure 2. Sketch of the bispectrum of the response, (12).

At third order, the bispectrum of the response is expressed by (12) at leading order. This function is represented in Figure 2 which illustrates the background component as a central peak of the frequency space as well as six peaks, coined as *biresonance peaks* as they correspond to resonance in two factors out of three in the each term of $B_x(\omega_1,\omega_2)$. These peaks are located at $(\omega_1,\omega_2)= (\pm\omega_o,0)$, $(0,\pm\omega_o)$ and $(\pm\omega_o,-\omega_o)$.

The background contribution to the integral in (13) is obtained by replacing the frequency response functions H_1 and H_2 by their local behaviour in Eq. (12), i.e. $H_1(\omega)=\rho C_d AU/k$ and $H_2(\omega_1,\omega_2)=\rho C_d A/2k$, which yields

$$\kappa_{3,B} = 3I_u \left(\frac{\rho C_d AU\sigma_u}{k} \right)^3 \tag{20}$$

Applying the procedure recommended in the multiple timescale spectral analysis, the additional contribution of the biresonance peaks is obtained as

$$\kappa_{3,R} = r\,\kappa_{3,B} \frac{2\xi_s + \xi_a}{\xi_s + \xi_a} \Psi_1 \tag{16}$$

with r the second-order resonant-to-background ratio introduced in (11) and

$$\Psi_1\left(S_u(\omega);\omega_o;\xi\right) = \int_{-\infty}^{+\infty} \frac{S_u(\omega)}{\sigma_u^2} \frac{4\xi^2\omega_o^2}{\omega^2 + 4\xi^2\omega_o^2} \mathrm{d}\omega \tag{17}$$

and where the shorter notation $\xi = \xi_s + \xi_a$ is used. The total cumulant of the response is finally written as the sum of the background and biresonant components, $\kappa_{3,B} + \kappa_{3,R}$.

The appreciable outcome of the method is that the order of integration to determine the third cumulant of the response has dropped from 2, in Eq. (13), to 1 in Eq. (17), as a result of the timescale separation.

A graphical representation of the trispectrum of the response (14) is a bit more involved as it concerns a function of three parameters. However the generic procedure developed at the third order may be replicated. It reveals the existence of four types of peaks, namely (i) a background peak located at the origin, as usual, (ii) four *A*-type mixed background-resonant peaks located in $(\omega_1,\omega_2,\omega_3)=\pm(\omega_o ,0,-\omega_o)$ and $(\omega_1,\omega_2,\omega_3)=(\omega_o,\pm\omega_o,0)$, (iii) two *B*-type mixed background-resonant peaks located at $(\omega_1,\omega_2,\omega_3)=\pm(0, \omega_o,-\omega_o)$ and (iv) four (purely) resonant peaks located at $(\omega_1,\omega_2,\omega_3)=\pm(\omega_o,\omega_o,-\omega_o)$ and $(\omega_1,\omega_2,\omega_3)=\pm(\omega_o,-\omega_o,-\omega_o)$.

The natures of these peaks are different because they each maximize different factors in the expression of the trispectrum. To keep it simple, the background peak corresponds to the only possible value of $(\omega_1, \omega_2, \omega_3)$ that maximizes the factors in S_u, while the four resonant peaks correspond to the four possible combinations of $(\omega_1, \omega_2, \omega_3)$ that maximize three out of the four factors in H_1 or H_2. Mixed A- and B-type peaks maximize one (or two) factors in H_1 or H_2 and two (resp. one) factors in S_u.

Resorting again to the basic principles of the multiple timescale spectral analysis (Denoël, 2014), the integral in Eq. (15) can be approximated by the sum of the four terms:

$$\begin{aligned}
&\kappa_{4,B} = 12I_u^2 \left(\frac{\rho C_d AU\sigma_u}{k} \right)^4; &&\kappa_{4,BR_I} = r\,\kappa_{4,B} \frac{2\xi_s + \xi_a}{\xi_s + \xi_a} \Psi_1; \\
&\kappa_{4,BR_{II}} = r\,\kappa_{4,B} \left(\Psi_2 - \frac{\xi_a}{\xi_s + \xi_a} \Psi_3 \right); &&\kappa_{4,R} = r^2\,\kappa_{4,B} \frac{\xi_s + \frac{\xi_a}{2}}{\xi_s + \xi_a} \Psi_1
\end{aligned} \tag{18}$$

with $\Psi_2(S_u(\omega);\omega_o;\xi)$ and $\Psi_3(S_u(\omega);\omega_o;\xi)$ are defined as

$$\Psi_2 = \int_{-\infty}^{+\infty}\int_{-\infty}^{+\infty} \frac{S_u(\omega_1)}{\sigma_u^2} \frac{S_u(\omega_2)}{\sigma_u^2} \frac{4\xi^2\omega_o^2}{(\omega_1 - \omega_2)^2 + 4\xi^2\omega_o^2} \mathrm{d}\omega_1\,\mathrm{d}\omega_2 \tag{19}$$

$$\Psi_3 = \int_{-\infty}^{+\infty}\int_{-\infty}^{+\infty} \frac{S_u(\omega_1)}{\sigma_u^2} \frac{S_u(\omega_2)}{\sigma_u^2} \frac{2\xi^2\left[32\xi^4\omega_o^4 + \omega_1\omega_2\left(8\xi^2\omega_o^2 + (\omega_1-\omega_2)^2\right)\right]}{\left(\omega_1{}^2 + 4\xi^2\omega_o^2\right)\left(\omega_2{}^2 + 4\xi^2\omega_o^2\right)\left((\omega_1-\omega_2)^2 + 4\xi^2\omega_o^2\right)} \mathrm{d}\omega_1\,\mathrm{d}\omega_2 \tag{20}$$

In our formulation, integrals are hidden in the coefficients Ψ_1, Ψ_2 and Ψ_3, but the dimensionality of the integrals is limited to 2, or even to 1 when mixed background-resonant components are dropped (which unfortunately degrades the quality of the result, see Denoël, 2012).

3.2 Skewness and Excess Coefficients

The skewness and excess coefficients of the response are readily obtained from the corresponding cumulant. With the multiple timescale approximation, they read

$$\gamma_3 = 3I_u \frac{1 + r\dfrac{2\xi_s + \xi_a}{\xi_s + \xi_a}\Psi_1}{\left(1+r\right)^{3/2}}; \quad \gamma_e = 12I_u^2 \frac{1 + r\left(\dfrac{2\xi_s + \xi_a}{\xi_s + \xi_a}\Psi_1 + \Psi_2 - \dfrac{\xi_a}{\xi_s + \xi_a}\Psi_3\right) + r^2 \dfrac{\xi_s + \dfrac{\xi_a}{2}}{\xi_s + \xi_a}\Psi_1}{\left(1+r\right)^2} \quad (21)$$

What this model offers is a simple and attractive procedure for the computation of the skewness and excess coefficients of the nonlinear response of the considered problem. These coefficients are simply expressed as a function of the resonant-to-background ratio denoted by r, the damping coefficients, structural and aerodynamic, as well as the coefficients Ψ_1, Ψ_2 and Ψ_3 which holds the remaining computational issues.

Interestingly enough, these latter coefficients have closed-form asymptotic expressions, for large and small values of the total damping coefficient. The relative smallness has to be assessed by comparison with the ratio of the characteristic frequency of the wind velocity turbulence and that natural frequency of the structure, α introduced in (2). For instance, one may observe that all three factors tend to 1 when $\xi \gg \alpha$. This makes the estimation of the skewness and excess coefficients of the response promptly accessible.

The amplitude of the nonlinearity scales with the magnitude of the aerodynamic damping, see (2). For small values of that parameter, the response is still non-Gaussian as a result of the square transformation of the wind velocity turbulence u^2. In the limit case, the structural behavior is linear and the current formulation degenerates into existing approximation based on the multiple timescale spectral analysis too (Denoël, 2011). What mainly matters here is that the non-Gaussianity of the response (measured by the magnitude of the skewness and excess coefficients) decreases as some nonlinear feedback is injected into the structure. This is readily observed by substituting ξ_a by 0 in Eqs. (21); the coefficients of Ψ_1, Ψ_2 and Ψ_3 are systematically decreased. This validates the following statement. The differentiation in the feedback loop acts as a high-pass filter of the structural response. It is well known that the non-Gaussianity of the response mainly results from the low-frequency content while the resonant component of the response is simply Gaussian. Consequently the correction to the open-loop system is more or less Gaussian and this tends to diminish the non-Gaussianity of the loading. The model described in this paper is a simple tool to quantify this return to the Gaussian distribution.

The few details that were communicated in this paper are not really sufficient to understand that the local approximations of the kernel, that allowed the derivation of the low-dimensional integral solutions, are actually not affected by the presence of the square velocity feedback. In other words, the squared structural velocity $\dot{x}^2(t)$ term is definitely negligible in front of the parametric excitation $-2\dot{x}(t)u(t)$ term, no matter the values and relative smallness of the parameters of this problem. The only limitation on this observation is that the timescales remain well separated.

At last but not least, another interesting case is that of a small dynamic amplification, in the second-order sense, i.e. $r \ll 1$. In that case, both the mixed and resonant contributions vanish and the skewness and excess coefficients of the response match those of the quadratic transformation of the Gaussian wind velocity turbulence, i.e. $\gamma_3 = 3I_u$ and $\gamma_e = 12I_u^2$.

4 Numerical application

A Monte Carlo simulation of the original nonlinear system (1) and of its 2nd-order Volterra series approximation (5) provides realizations of the total response $x(t)$, as well as of the terms $x_1(t)$ and $x_2(t)$

of the Volterra series approximation. With the help of an online averaging method, the raw moments of $x(t)$, $x_1(t)$, $x_2(t)$ are readily obtained. They are finally translated into cumulants, as they offer a more convenient understanding. Figure 3 shows the comparison of the skewness (a) and coefficient of excess (b) of the full nonlinear response $x(t)$ (blue surface) and its Volterra series approximation $x_1(t)+x_2(t)$ (red surface). It can observed that, within the considered parameter space, the 2nd-order Volterra system provides a perfect representation of the skeness and a slight overestimation of the coefficient of excess. Figure 4 shows the comparison, again in terms of skewness (a) and coeffient of excess (b), of the solution provided by the numerical integration of the 2nd-order Volterra series (blue surface) and by the proposed analytical solution (red surface). The analytical solution provides a good estimation of skewness, while tends to overestimate a bit the numerical results. A good agreement is observed in the region of high aerodynamic damping and low structural damping, which is the most relevant from a technical point of view.

As far as the computational efficiency is concerned, it should be emphasized that the analytical solution is extremely convenient when the two timescales involved in the problem are very different from each other, i.e. α is small. In this case, indeed, the Monte Carlo simulation requires the integration of very long time series using a small time step. For example, the computation of the results shown in Figures 3 and 4 (400 points of the parameters space) required about five minutes for the analytical solution and about 2500 hours CPU time for the Monte Carlo simulation (mostly used for the solution of the full nonlinear system).

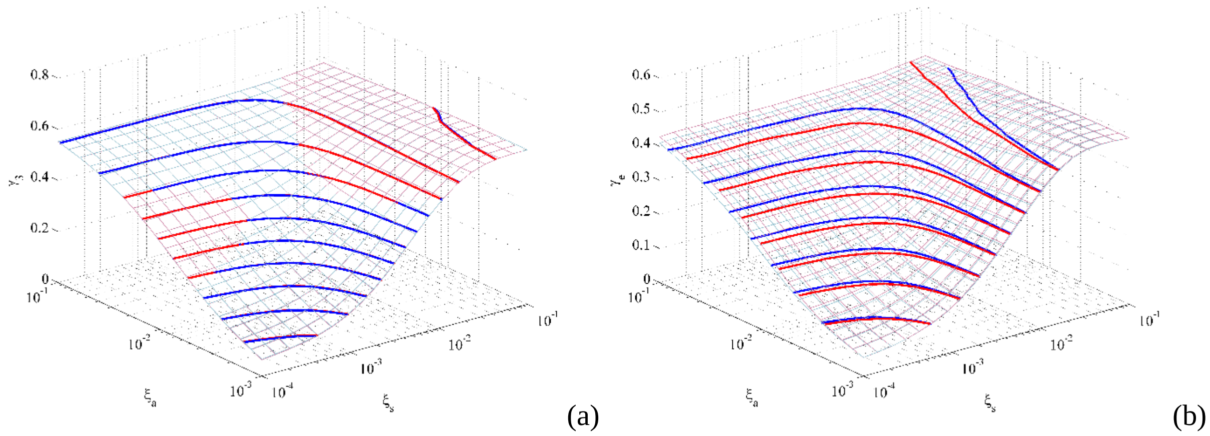

Figure 3. Skewness (a) and coefficient of excess (b) of full nonlinear response (blue) and 2nd-order Volterra series approximation (red).

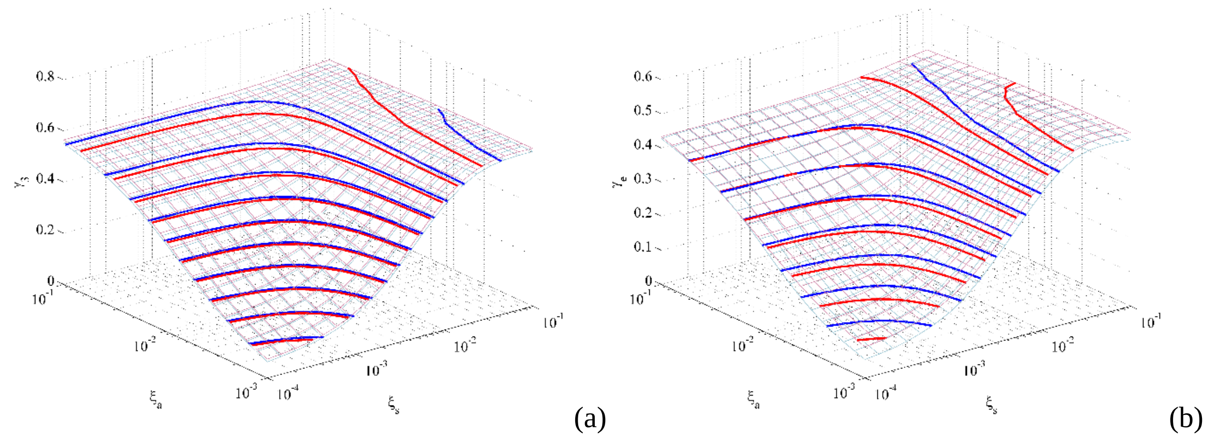

Figure 4 Skewness (a) and coefficient of excess (b) of 2nd-order Volterra series approximation (blue) and analytical solution (red).

5 Conclusions

There are two main contributions in this paper. The first one concerns the derivation of the very general solution, expressed as accurate approximations though, of the stochastic response of a second-order Volterra model. Equations presented in this paper are rather general and might be applied in other fields or problems, as long as the timescales separation hypothesis holds.

The second contribution concerns the application to a classical problem of wind engineering, namely the influence of the nonlinear quadratic velocity and parametric loading terms arising in a quasi-steady aerodynamic loading. Although not given with full details, the derivation demonstrates that the parametric loading term is mainly responsible for the non-Gaussianity of the response, while the squared structural velocity term has very few influence. As an interesting outcome too, it is demonstrated that the nonlinear quadratic velocity feedback systematically reduces the skewness and excess coefficients of the loading.

References

Davenport , A. G. (1961). The application of statistical concepts to the wind loading of structures. *Proceedings of the Institute of Civil Engineers* **19**, 449-472.

Denoël, V. (2014), Multiple Timescale Spectral Analysis. *Probabilistic Engineering Mechanics*. *Submitted*.

Schetzen, M. (1980). *The Volterra and Weiner theories of nonlinear systems*. John Wiley & Sons, Inc., New York.

Carassale, L. and Kareem A. (2010). Modeling nonlinear systems by Volterra Series. *Journal of Engineering Mechanics* ASCE **136**, 801-818.

Bedrosian, E. and Rice S. O. (1971). Output properties of Volterra systems (nonlinear systems with memory) driven by harmonic and Gaussian inputs. *Proceedings of the IEEE* **59**(12), 1688-1707.

Papoulis, A. (1965). *Probability, Random Variables, and Stochastic Processes*. New York, McGraw Hill.

Denoël, V. and Carassale L. (2014). Response of an oscillator to a random quadratic velocity-feedback loading. *Under preparation*.

Feijoo, J. A. V., Worden, K. and Stanway, R. (2005). Associated linear equations for Volterra operators. *Mechanical Systems and Signal Processing* **19**(1): 57-69.

Denoël, V. (2011). On the background and biresonant components of the random response of single degree-of-freedom systems under non-Gaussian random loading. *Engineering Structures* **33**(8): 2271-2283.

Denoël, V. (2012). Extension of the Background/biResonant decomposition to the estimation of the kurtosis coefficient of the response. *Uncertainty in Structural Dynamics 2012. Leuven, Belgium.*